

This poster builds upon the earlier work of Osborn *et al.* (1999), Ulbrich *et al.* (1999), Zorita & Gonzalez-Ruoco (2000) and others, in evaluating and applying climate model simulations to answer a number of questions about the North Atlantic Oscillation. This study expands the comparison to include six different global climate models, and is being written up with full details and an extended discussion for submission to a scientific journal. Throughout this work, seasonal-mean winter (December to March) sea level pressure (SLP) data are used, and the North Atlantic Oscillation and its index are defined as the leading empirical orthogonal function (EOF) and associated principal component (PC) time series of the Atlantic half of the Northern Hemisphere SLP field.

The **first column** (hPa) of maps shows how well the models reproduce the winter SLP climatology (see also the pattern correlation values at the right-hand side). The large scale features are reasonably simulated, though their absolute values are sometimes in error. The leading mode of Atlantic-sector interannual variability (**column two**, expanded to give hemispheric patterns), defined by the leading EOF of SLP from each model's

control run, is clearly the NAO in all cases. Projecting observed SLP onto the simulated EOFs results in time series that closely match the observed leading PC, indicating that biases in the simulated NAO patterns are relatively unimportant. Nevertheless, they are interesting, with the main bias being a tendency for enhanced correlation with the North Pacific SLP in some models (becoming closer to an Arctic Oscillation, despite being defined using only Atlantic-sector SLP). In most models, this leading EOF explains more variance than is the case for the observations.

If we keep this definition of the NAO constant, and then project the SLP from simulations with increasing greenhouse gas concentrations (g1 simulations) onto the control run EOFs, we yield the time series shown below. All six models indicate increasing values of the NAO index, though with varying magnitude. The reason for these trends is that there is a long-term trend in the SLP patterns in all models when enhanced greenhouse forcing is applied (**column three**, hPa per century), which either resembles the NAO (e.g., CCSR/NIES, ECHAM4/OPYC, NCAR PCM, and HadCM3) or at least has some power over the

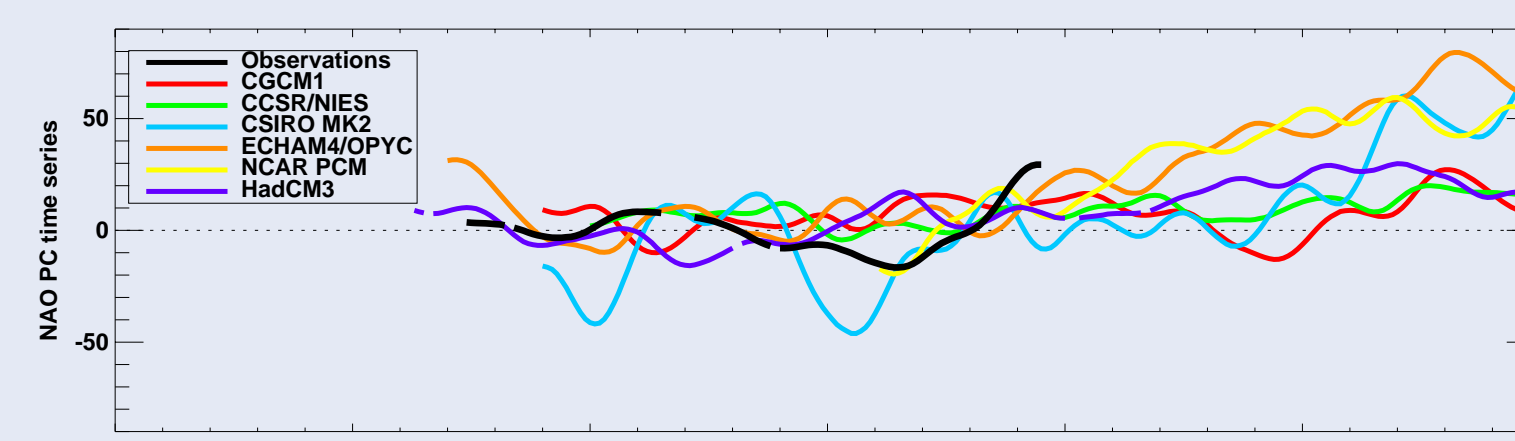
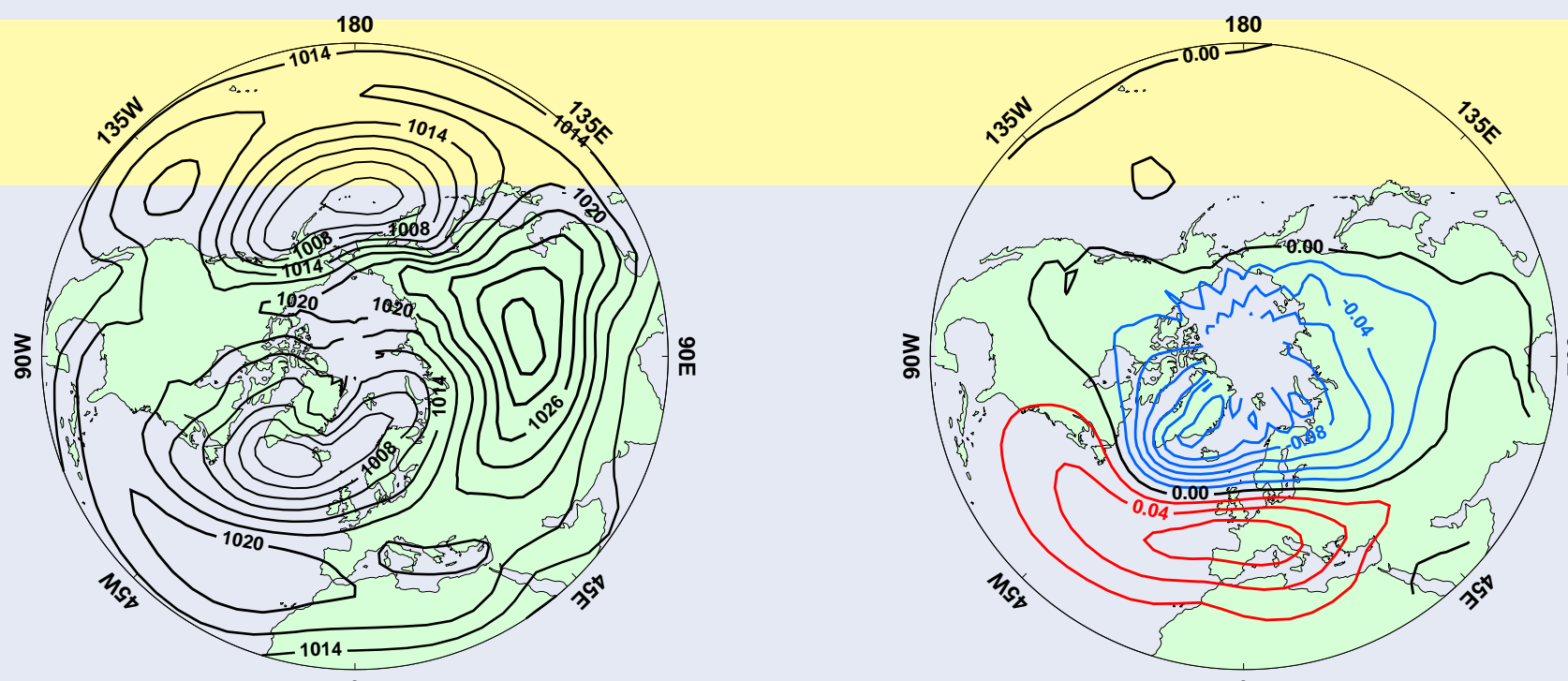
NAO centres of action.

An alternative approach (e.g., Ulbrich & Christoph, 1999) is to allow the NAO definition to alter and diagnose how the oscillation itself may change under enhanced greenhouse forcing. The **fourth column** indicates the EOFs of the (detrended) SLP field computed from the 2050-2099 period of the g1 simulations. Under the altered forcing, the NAO explains a similar amount of variance (when considering all models together), though the interannual variability may be lower. The EOF patterns show a number of changes: for CCSR/NIES, CSIRO MK2, ECHAM4/OPYC and HadCM3, the Azores centre of action shifts eastward (and slightly northward), while for CGCM1 and ECHAM4/OPYC the Iceland centre of action shifts eastward. CCSR/NIES, ECHAM4/OPYC and NCAR PCM show an intensification of the Azores centre of action, while CGCM1 and HadCM3 show the reverse.

Further work is in progress, assessing temporal variability changes and comparing recent observed NAO changes with the range of variability simulated by the climate models (see, e.g., Osborn *et al.*, 1999).

Observations

UKMO sea level pressure analyses 1873-1995 (Jones, 1987; Basnett & Parker, 1997)



Smoothed time series showing the NAO indices from the greenhouse gas forced simulations, when their SLP fields are projected onto the corresponding control run NAO patterns. Observed NAO time series is also shown.

Statistics given for each model

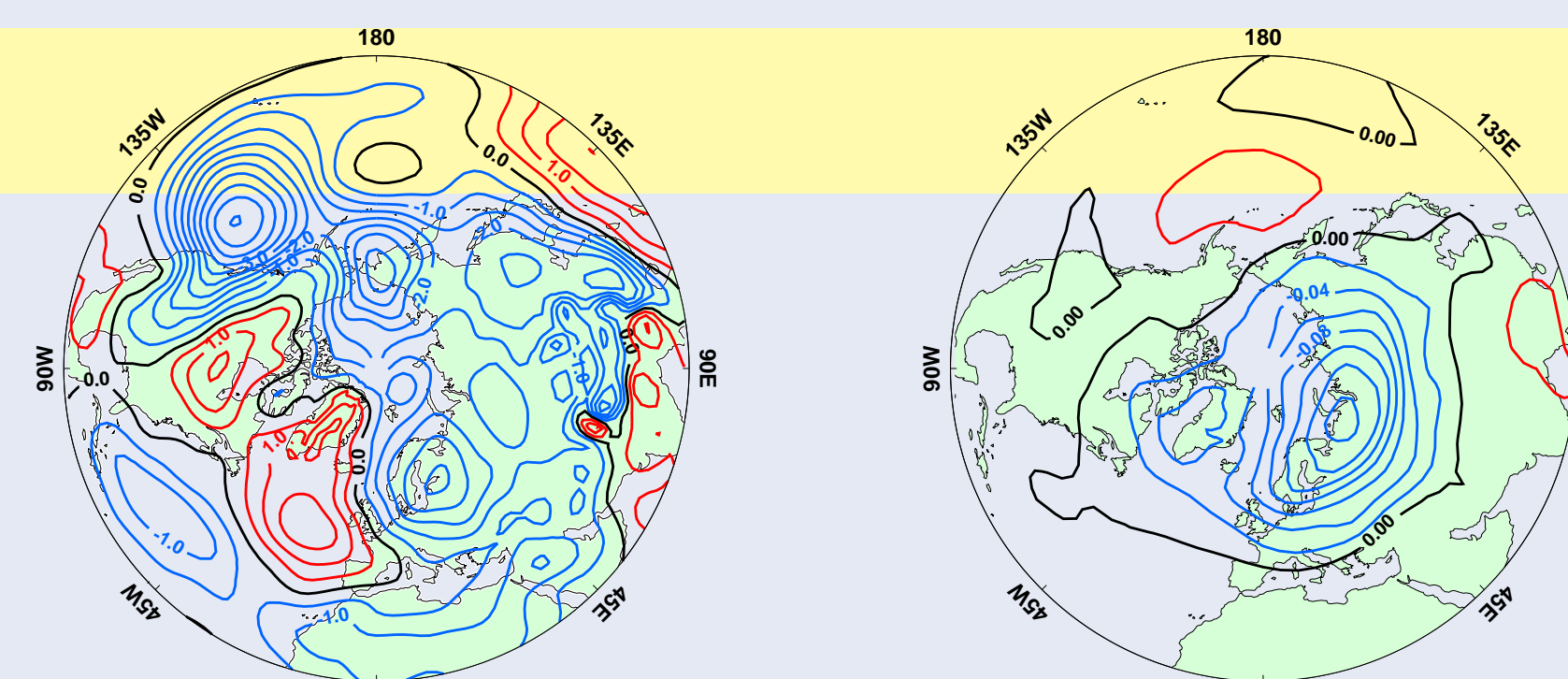
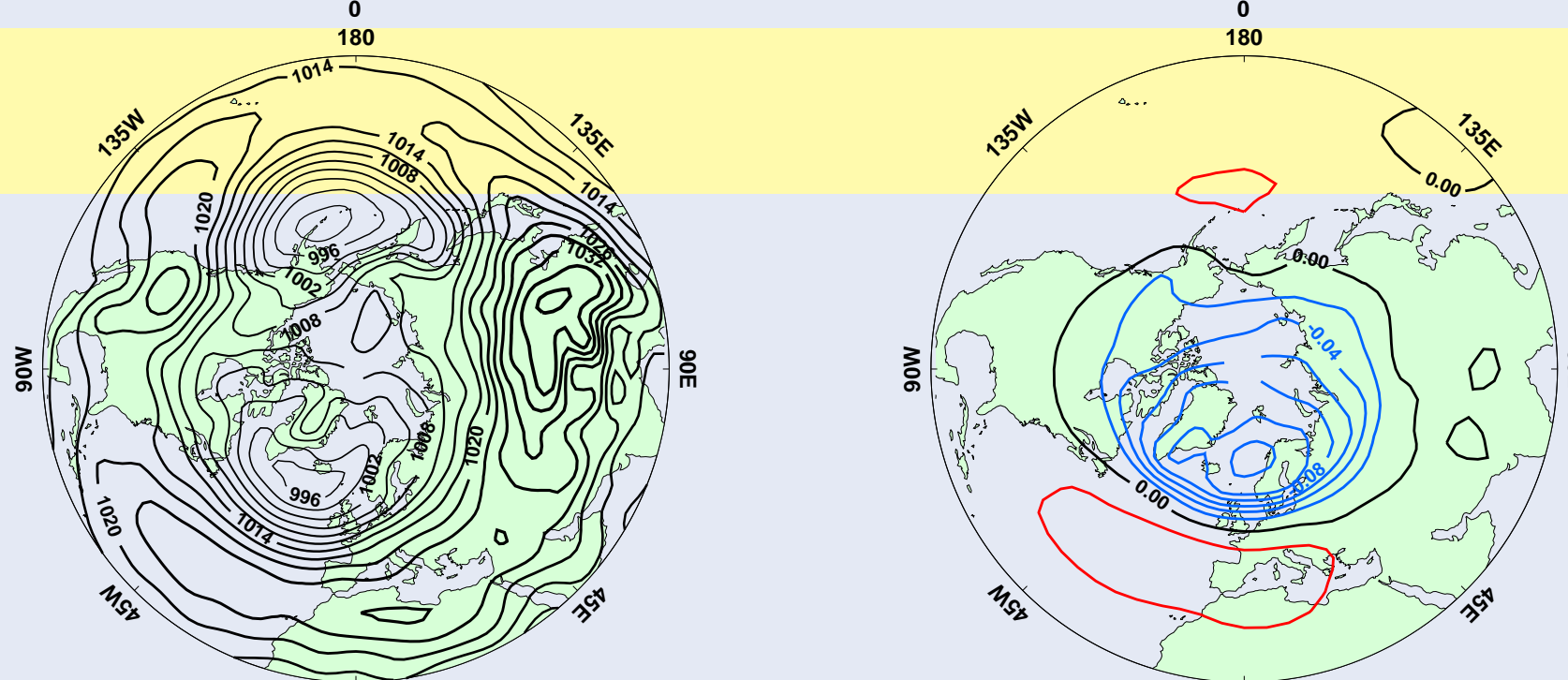
pattern: pattern correlation between observed and simulated mean SLP

% con: percentage of Atlantic SLP variability explained by EOF1 during the control (observed value is 40%)

% g1: percentage of Atlantic SLP variability explained by EOF1 during the g1 simulation

CGCM1

Canadian Center for Climate Modelling and Analysis, Canada. Model and simulations described by Flato *et al.* (2000).

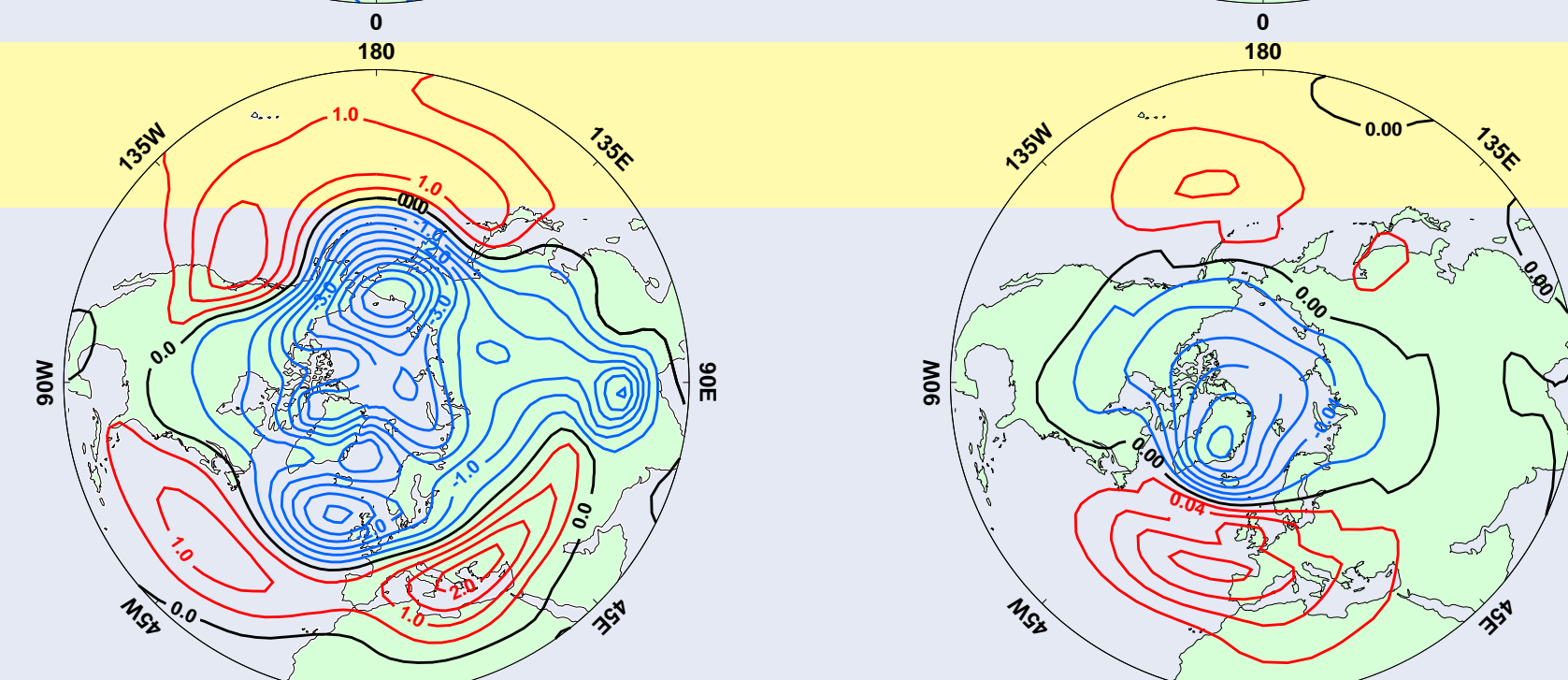
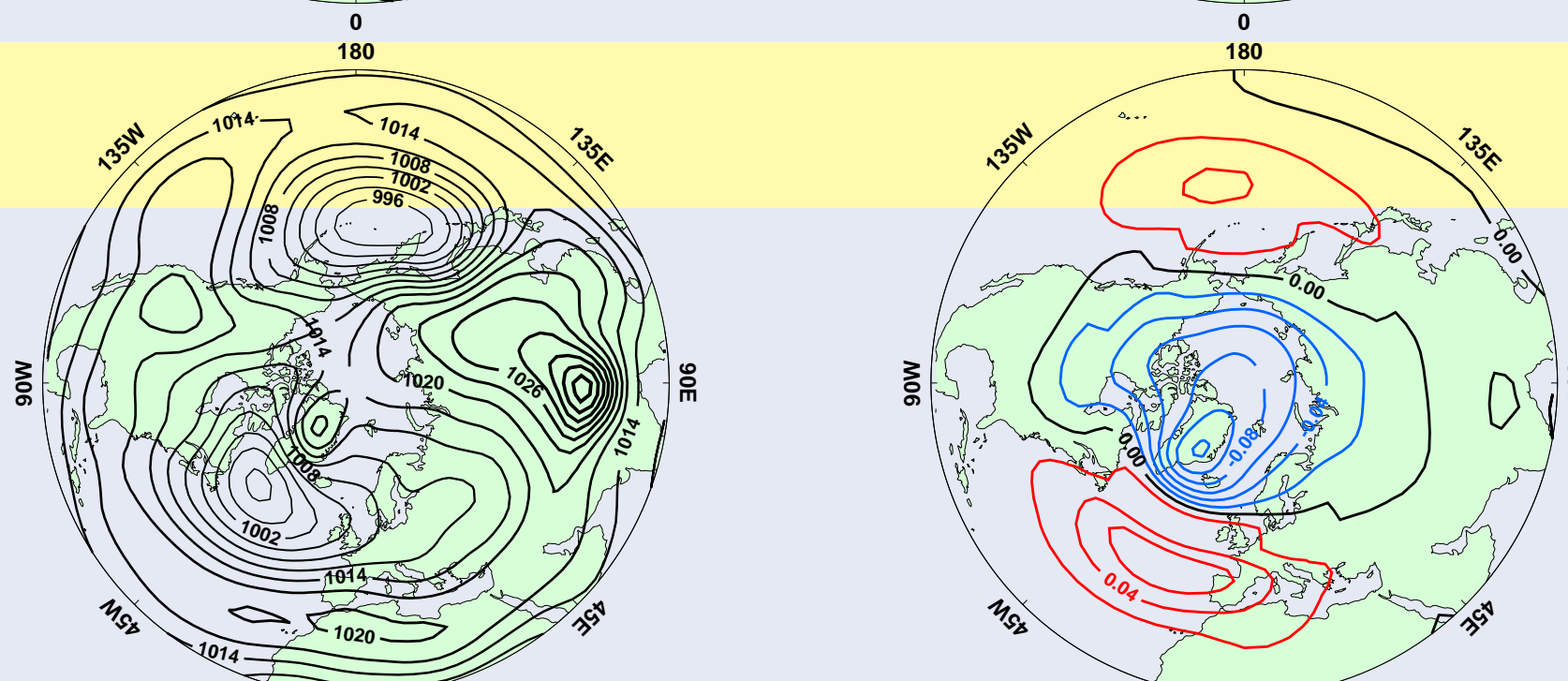


CGCM1

pattern: 0.79
% con: 56
% g1: 42

CCSR/NIES

Center for Climate Research Studies and National Institute for Environmental Studies, Japan. Model and simulations described by Emori *et al.* (1999).

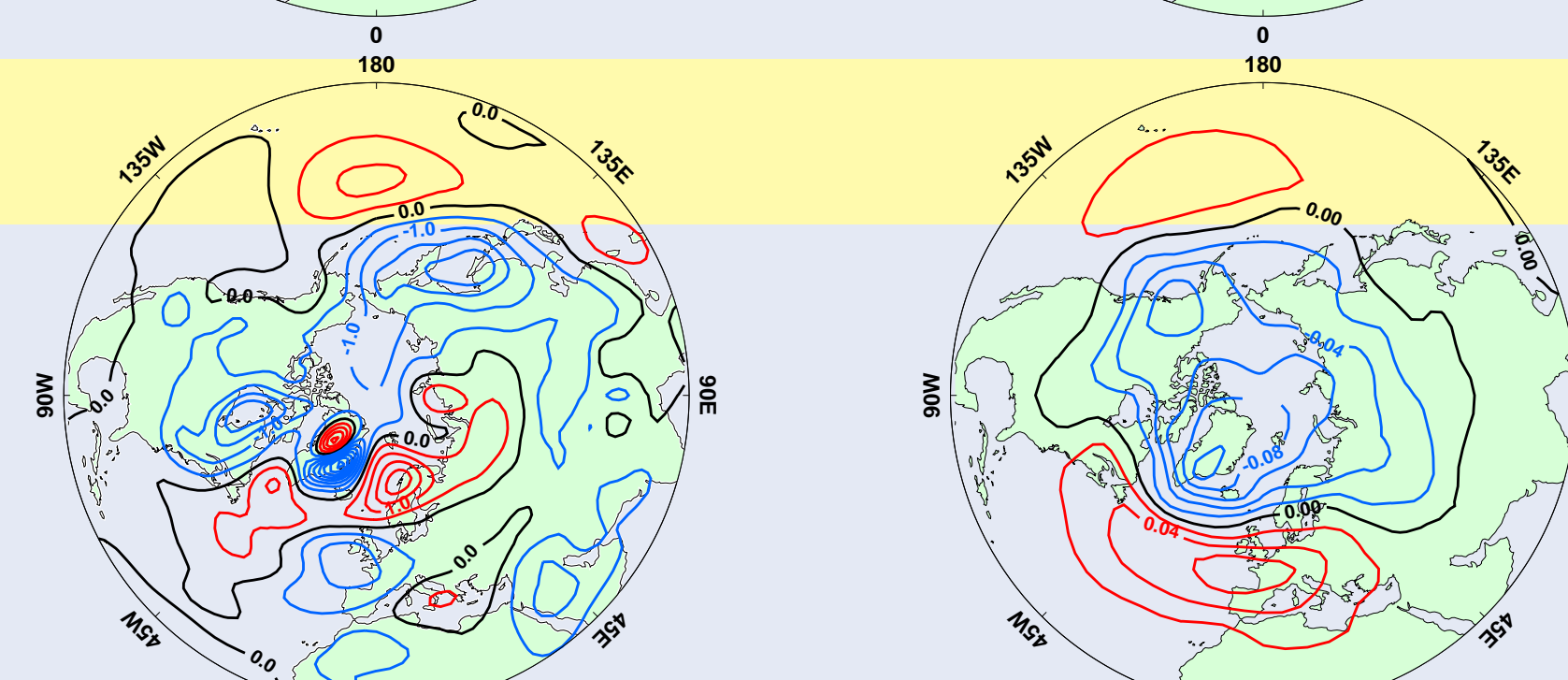
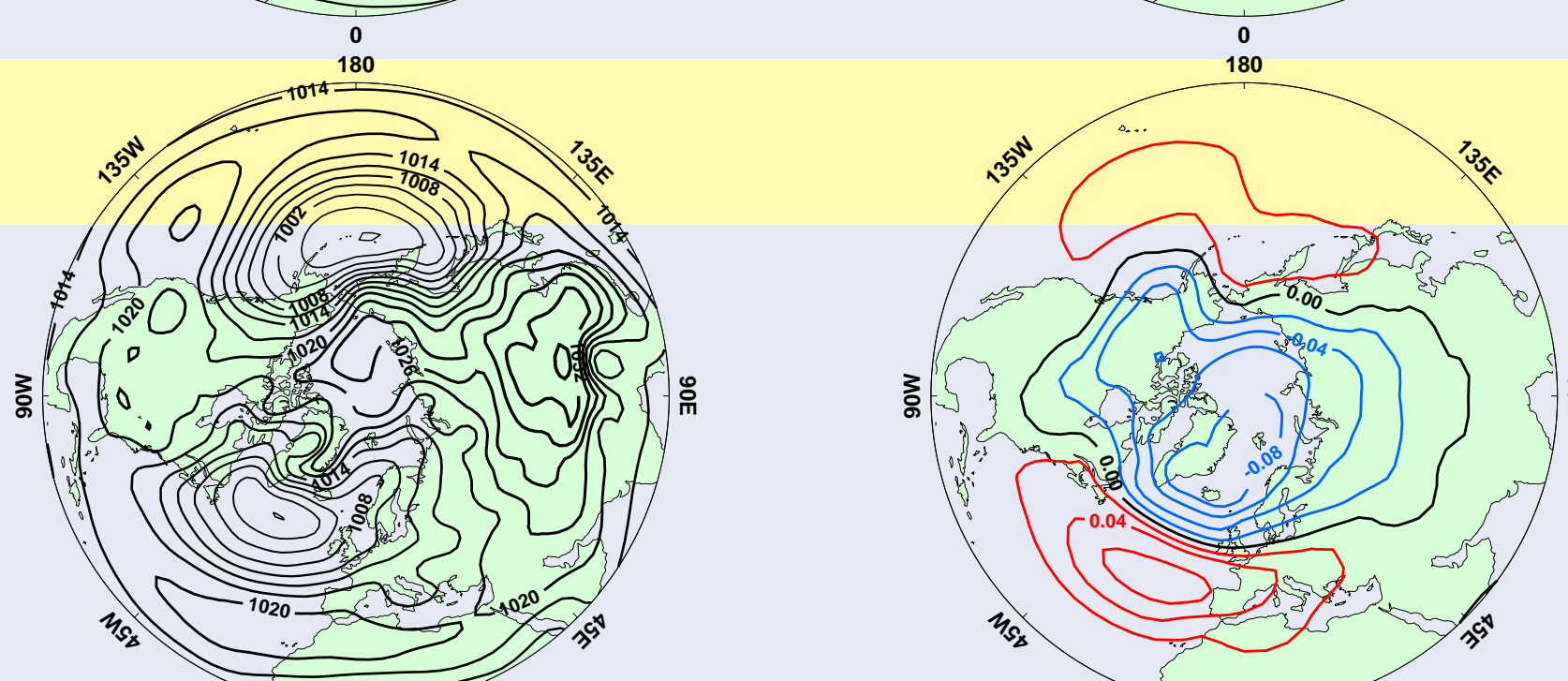


CCSR/NIES

pattern: 0.76
% con: 66
% g1: 71

CSIRO MK2

Commonwealth Scientific and Industrial Research Organisation, Australia. Model and simulations described by Gordon & O'Farrell (1997).

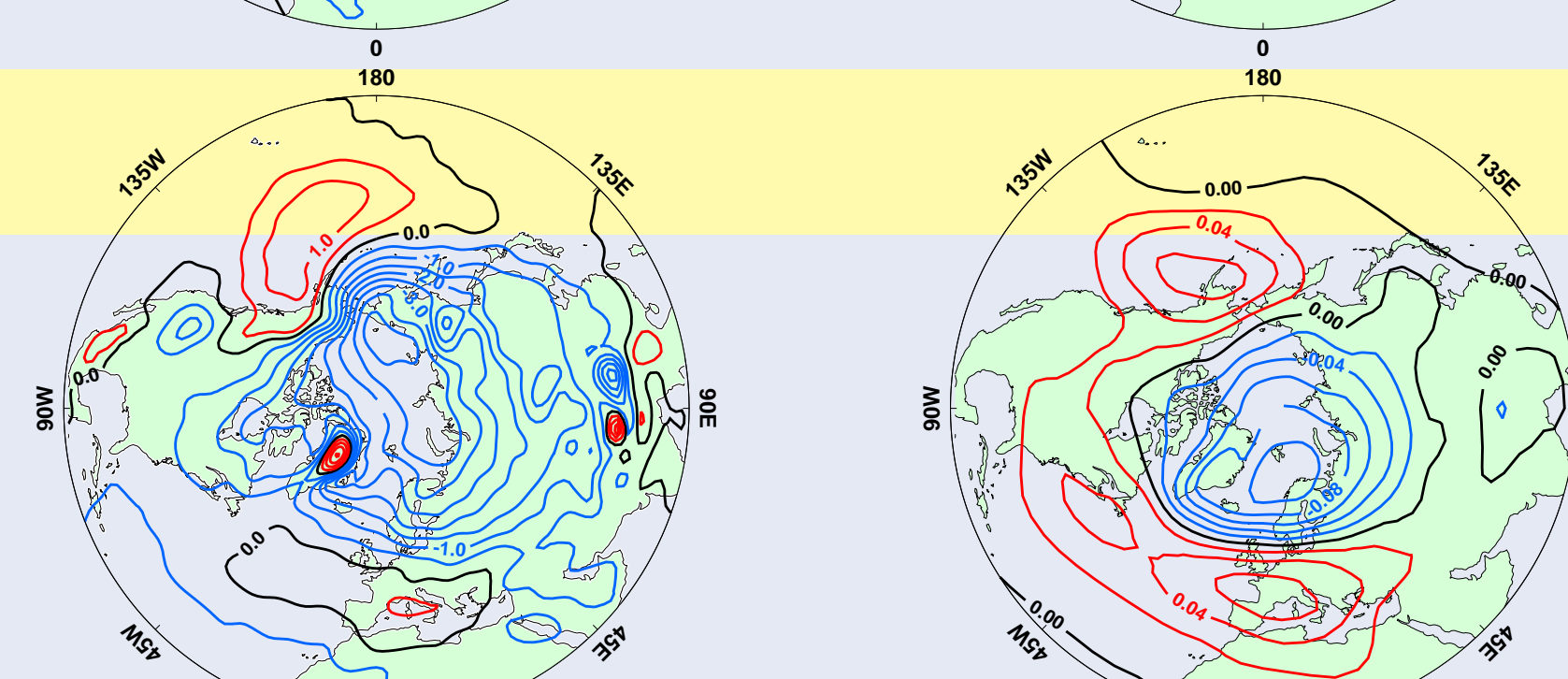
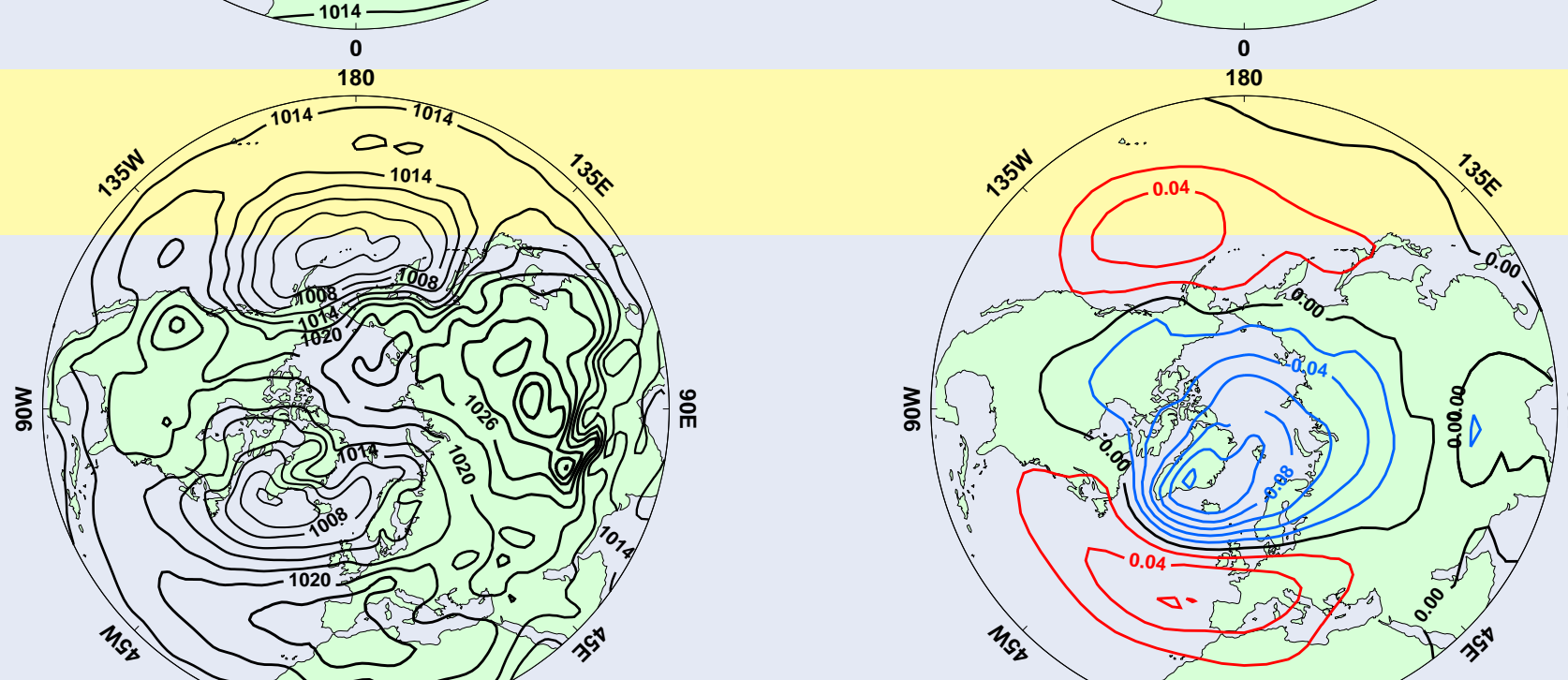


CSIRO MK2

pattern: 0.81
% con: 40
% g1: 42

ECHAM4/OPYC

Deutsches Klimarechenzentrum DKRZ, Germany. Model and simulations described by Bacher *et al.* (1998).

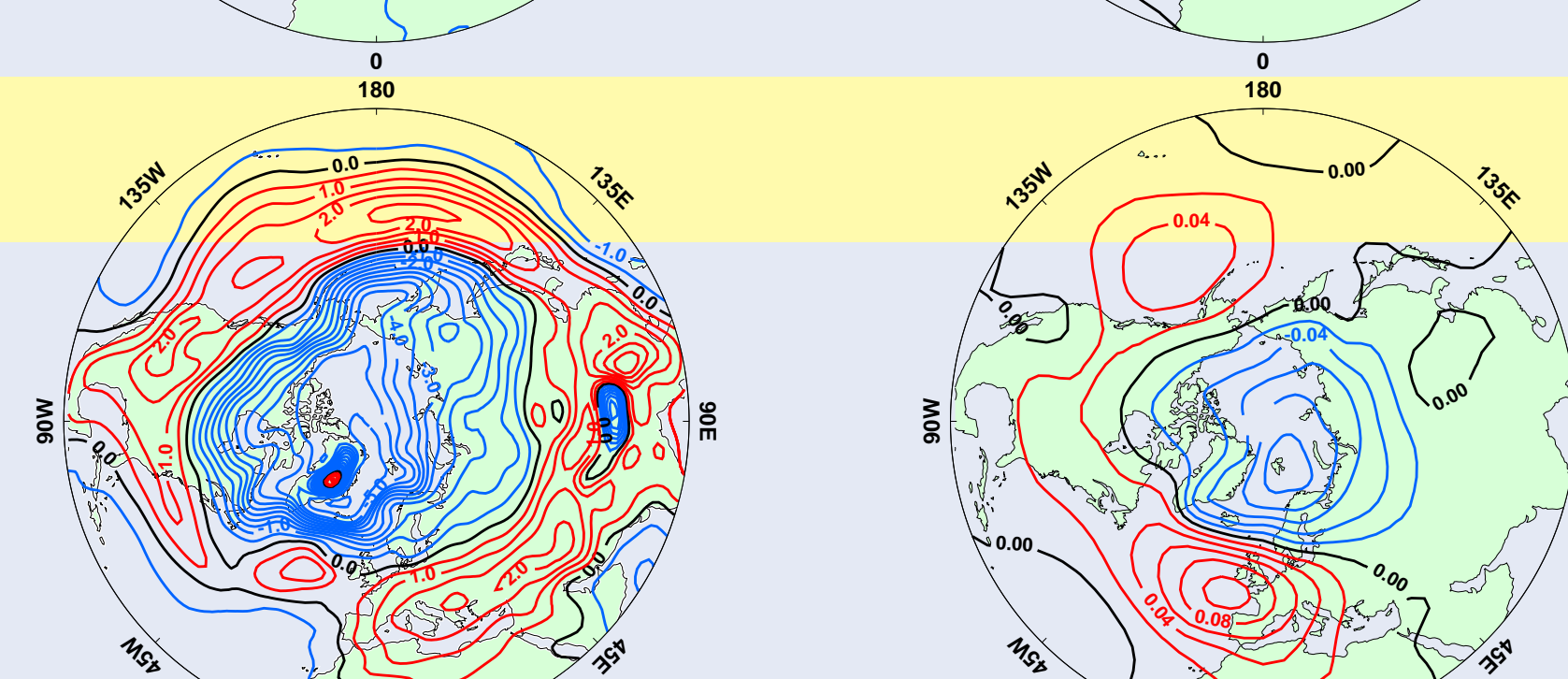
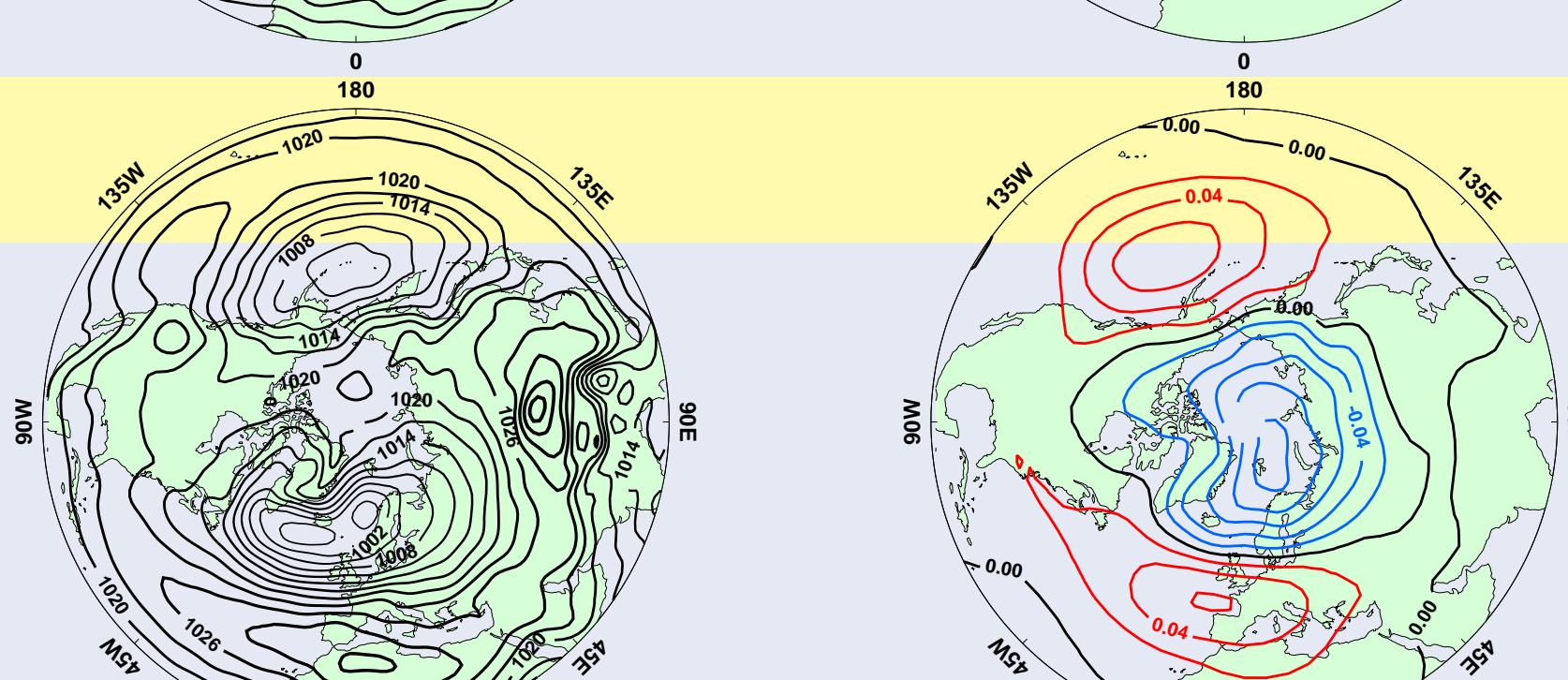


ECHAM4/OPYC

pattern: 0.88
% con: 55
% g1: 47

NCAR PCM

National Centre for Atmospheric Research, USA. Model and simulations described by Washington *et al.* (2000).

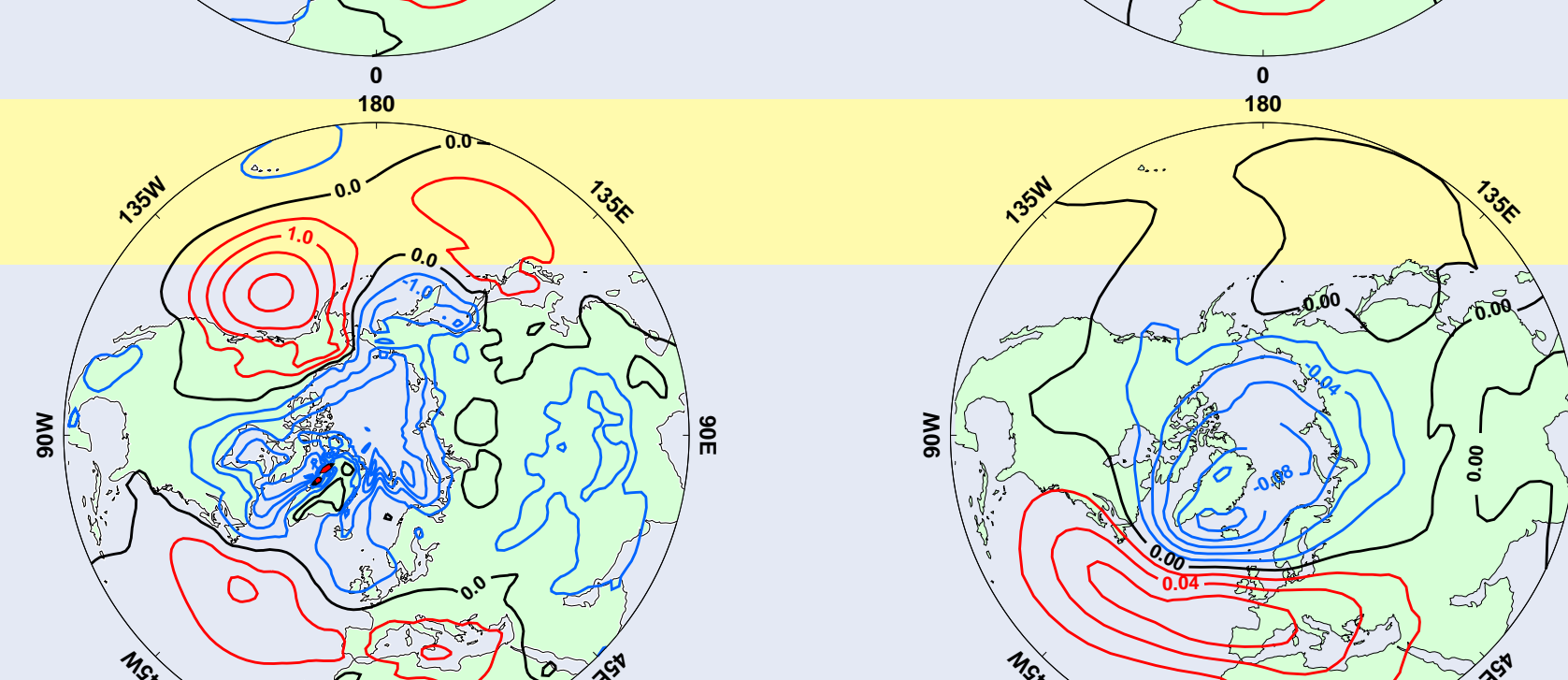
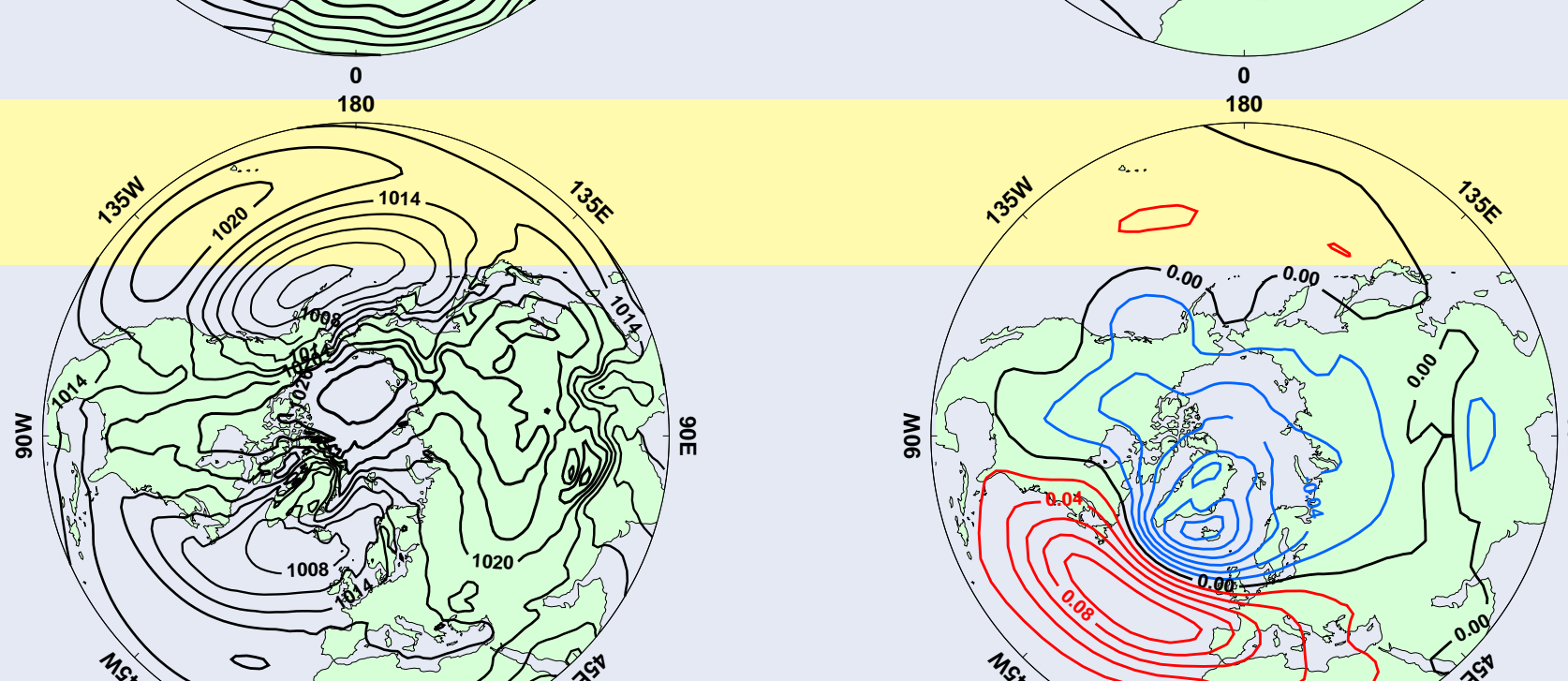


NCAR PCM

pattern: 0.85
% con: 53
% g1: 50

HadCM3

Hadley Centre for Climate Prediction and Research, UK. Model and simulations described by Gordon *et al.* (2000).



HadCM3

pattern: 0.67
% con: 44
% g1: 48

References

Bacher A, Oberhuber JM & Roeckner E (1998) ENSO dynamics and seasonal cycle in the tropical Pacific as simulated by the ECHAM4/OPYC3 coupled general circulation model. *Climate Dynamics* **14**, 431-450.
Emori S, Nosawa T, Abe-Ouchi A, Numaguti A, Kimoto M & Nakajima T (1999) Coupled ocean-atmosphere model experiments of future climate change with an explicit representation of sulfate aerosol scattering. *J. of the Meteorological Society of Japan* **77**, 1299-1307.
Flato GM, Boer GJ, Lee WG, McFarlane NA, Ramsden D, Reader MC & Weaver AJ (2000) The Canadian Centre for Climate Modelling and Analysis global coupled model and its climate. *Climate Dynamics* **16**, 451-467.
Gordon C, Cooper C, Senior CA, Banks H, Gregory JM, Johns TC, Mitchell JFB & Wood RA (2000) The simulation of SST, sea ice extents and ocean heat transports in a version of the Hadley Centre coupled model without flux adjustments. *Climate Dynamics* **16**, 147-168.
Gordon HB & O'Farrell SP (1997) Transient climate change in the CSIRO coupled model with dynamic sea ice. *Monthly Weather Review* **125**, 875-907.
Osborn TJ, Briffa KR, Tett SFB, Jones PD & Trigo RM (1999) Evaluation of the North Atlantic Oscillation as simulated by a coupled climate model. *Climate Dynamics* **15**, 685-702.
Ulbrich U & Christoph M (1999) A shift of the NAO and increasing storm track activity over Europe due to anthropogenic greenhouse gas forcing. *Climate Dynamics* **15**, 551-559.
Washington WM, Weatherly JW, Meehl GA, Semtner Jr AJ, Bettge TW, Craig AP, Strand Jr WG, Arblaster JM, Wayland VB, James R & Zhang Y (2000) Parallel Climate Model (PCM) control and transient simulations. *Climate Dynamics* **16**, 755-774.
Zorita E & Gonzalez-Ruoco (2000) Disagreement between predictions of the future behaviour of the Arctic Oscillation as simulated in two different climate models: implications for global warming. *Geophysical Research Letters* **27**, 1755-1758.

Acknowledgements

This work was supported by the UK Natural Environment Research Council (NERC GR3/12107). Climate model output was obtained via the Climate Impacts LINK Project (UK DETR EPG 1/1/68) on behalf of the Hadley Centre, and via the IPCC Data Distribution Centre.